TECHNICAL REPORT R-48

A SYSTEMATIC KERNEL FUNCTION PROCEDURE FOR DETERMINING AERODYNAMIC FORCES ON OSCILLATING OR STEADY FINITE WINGS AT SUBSONIC SPEEDS

By CHARLES E. WATKINS, DONALD S. WOOLSTON, and HERBERT J. CUNNINGHAM

Langley Research Center
Langley Field, Va.

TECHNICAL REPORT R-48

A SYSTEMATIC KERNEL FUNCTION PROCEDURE FOR DETERMINING AERODYNAMIC FORCES ON OSCILLATING OR STEADY FINITE WINGS AT SUBSONIC SPEEDS

By Charles E. Watkins, Donald S. Woolston, and Herbert J. Cunningham

SUMMARY

A detailed description is given of a method of approximating solutions to the integral equation that relates oscillatory or steady lift and downwash distributions on finite wings in subsonic flow. The method of solution is applicable to general plan forms with either curved or straight leading and trailing edges. Moreover, it is directly applicable to control surfaces such as all-movable tails but modifications are needed to apply it to controls in general. Applications of the method involve evaluations of numerous integrals that must be handled by numerical procedures but systematic schemes of evaluations have been adopted that are well suited to the routines of automatic digital computing machines. These schemes of evaluation have been incorporated in a program for an IBM 704 electronic data processing machine. With this machine, a pressure distribution together with such quantities as section or total lift and moment coefficients or generalized forces can be determined for a given value of frequency and Mach number and for several (four or five) modes of oscillation in about 4 minutes of machine time. In the case of steady downwash conditions corresponding quantities can be obtained in about 2 minutes of machine time.

In order to illustrate applications of the method, results of several calculations are presented. In these illustrations total forces and moments are compared (1) with results of analytic procedures for a circular plan form with steady downwash conditions, (2) with results of other theories and with experiment for a rectangular plan form of aspect ratio 1 at a uniform angle of attack, and (3) with some experimental results for a rectangular plan form of aspect ratio 2 undergoing pitching and flapping oscillations. Also included in the illustrations are results of flutter calculations compared with experimental results for an all-movable control surface of aspect ratio 3.50 and for a cantilevered rectangular plan form of aspect ratio 5.04.

INTRODUCTION

The equations that provide a basis for most of the existing theoretical aerodynamics of lifting surfaces result from a linearization of boundary-value problems for velocity potentials. The linearizations, of course, involve restrictions in addition to that of neglecting viscosity, which is required in formulating the potential equations in the first place, but these restrictions are generally necessary in order to simplify the problems to tractable forms. A main advantage gained through linearization is the principle of superposition, inherent to linear differential equations, which means not only that a given problem may be broken down into a category of different problems, which separate such parameters as thickness, camber, and angle of attack, but, more significantly for present purposes, that the linearized boundary-value problem can be converted to an integral equation; furthermore, the linearized differential equation is satisfied not only by the velocity potential but also by the pressure or a pressure potential so that the integral equation can be formulated on the basis of either a velocity potential or a pressure potential.

Even with the simplification and advantages gained through linearization the lifting-surface problem for oscillating wings has been explicitly solved for only a very few special wing plan forms. These are the wing of infinite aspect ratio (refs. 1 to 3), the wing for which the flow normal to all edges is supersonic (ref. 4), the wing of vanishingly small

aspect ratio (refs. 5 and 6), and, for an incompressible fluid, the wing of circular plan form (refs. 7 to 9). Not only do these few solutions constitute a small category but the prospects of obtaining explicit solutions for more general or arbitrary plan forms are extremely dim. In view of computing equipment that is now available, however, there exists an excellent possibility of obtaining solutions appropriate to any plan form by approximate or numerical procedures that are satisfactory for engineering purposes. A reliable concept on which to base these procedures underlies such developments as those of Falkner (ref. 10) and Multhopp (ref. 11) relating to steady finite wings and that of Possio (ref. 12) relating to oscillating wings of infinite aspect ratio.

This concept pertains to the boundary-value problem for the pressure potential when expressed as an integral equation that relates a prescribed downwash distribution to an unknown lift distribution. It is simply that from a knowledge of the few known explicit solutions to the lifting-surface problems the general character of the lift distribution for various conditions can be surmised; hence, by assuming that its general character is known, the unknown lift distribution can be replaced by a sum of appropriately chosen modes of lift functions, each mode being weighted by a constant coefficient that must yet be determined. Employing this concept or procedure then allows the known downwash distribution to be expressed as a sum of definite integrals with the unknown coefficients appearing as factors of the integrals. The definite integrals, however, are extremely unwieldy and, in general, can be evaluated only by approximate or numerical methods; it is in this regard that various lifting-surface methods, based on the concept under discussion, have their basic differences (i.e., in regard to the scheme or method by which integrations are numerically accomplished). Falkner's procedure, which has been extended to an oscillating finite wing in an incompressible medium in reference 13 and to an oscillating finite wing in a compressible medium in reference 14, involves the use of certain numerical integrating schemes which, although relatively simple to employ, depend in part on two-dimensional aerodynamic considerations and are difficult to assess with regard to accuracy. In Multhopp's procedure, which has been considered for the oscillating case in references 15 to 19 and others, more straightforward integrating schemes are used than are employed in Falkner's method but Multhopp's method, as he implies, is devised on the basis of a compromise between accuracy of results and computing effort required. It must be recalled, however, that both the Falkner and Multhopp methods were formulated at a time when high-speed computing equipment was in an embryonic state of development. Fortunately, with present-day computing equipment, it is seldom necessary to sacrifice accuracy of results for savings in labor of calculation.

In the present report a method is described in which straightforward integrating schemes that are well suited to the routines of high-speed digital computing machines are employed. The integrations can be made as accurate as desired; the accuracy can be easily assessed by simply changing the density of steps. The method applies to wings with oscillatory downwash conditions as well as to wings with steady-state downwash conditions. It also applies, with appropriate modifications in chosen modes of lift and regions of integration, to supersonic speeds as well as to subsonic speeds; however, only subsonic speeds are considered herein. The procedure is applicable to general plan forms with either curved or straight leading and trailing edges. Although it is readily applicable to control surfaces such as all-movable tails, modifications would be needed to apply it to controls in general.

A brief discussion is presented of the integral equation under study; the terms of the equation are examined and put in convenient forms, and a suitable working form of the equation is obtained. The numerical processes involved in handling this working form of the integral equation are discussed in detail. Still left untreated are some problems concerning the optimum number and location of control points and the degree of convergence of the process. Results of applying the procedure are given for a variety of plan forms and conditions. These include determinations of aerodynamic forces and moments for some special conditions and applications to some flutter problems.

SYMBOLS

A	aspect ratio, $4l^2/S$
$A_n(\eta)$	spanwise loading function in lift distribution (eq. (13))
a	velocity of sound, ft/sec
a_{nm}	weighting factor in $A_n(\eta)$

b local wing semichord, ft

b_0 wing root semichord, ft

C_{L,q_j}, C_{M,q_j} complex total lift and pitching-moment coefficients associated with jth mode of oscillation; for example, $C_{L,q_j}=(C_{L,q_j})_r+i(C_{L,q_j})_i$

$|C_{L,q_j}|, |C_{M,q_j}|$ magnitudes of complex lift and pitching-moment coefficients; for example,

$$|C_{L,q_j}|=\sqrt{[(C_{L,q_j})_r]^2+[(C_{L,q_j})_i]^2}$$

$F(\eta)$ complete chordwise integral in working form of integral equation (eq. (28))

F_p complete chordwise integral at station p (eq. (35))

$f_n(\eta)$ chordwise integral which involves nth chordwise term in lift distribution (eq. (29))

$H(x,y,t)$ vertical displacement of wing surface, positive down, ft

$h_j(x,y)$ shape function of vertical displacement in jth mode

$I_1(ks|y-\eta|)$ modified Bessel function of first kind of first order

$I_{\mathrm{I}}, I_{\mathrm{II}}, I_{\mathrm{III}}, I_{\mathrm{IV}}$ portions of spanwise integral (eq. (32))

$K_1(ks|y-\eta|)$ modified Bessel function of second kind of first order

$K[M,k,x_0, s(y-\eta)]$ kernel function of integral equation, ft^{-2}

$\overline{K}[M,k,x_0, s(y-\eta)]$ modified kernel function (eq. (16))

$\overline{K}_\theta(M,k,\theta,\eta)$ modified kernel function in terms of angular chordwise coordinate θ (see eq. (24))

k reduced frequency, $b_0\omega/V$

L total lift, positive down, lb

$$L=\rho\frac{V^2}{2}S\sum_j\frac{q_j}{b_0}C_{L,q_j}$$

$L_1(ks|y-\eta|)$ modified Struve function of first order

$L(\theta,\eta)$ nondimensional lift function (eq. (10))

l wing semispan, ft

$l_n(\theta)$ nth chordwise pressure mode expressed in terms of angular chordwise variable θ (eq. (12))

$\bar{l}_n(\xi)$ nth chordwise pressure mode expressed in algebraic form (eq. (14))

M Mach number

M_α total pitching moment, positive nose up, ft-lb

$$M_\alpha=\rho\frac{V^2}{2}Sb_0\sum_j\frac{q_j}{b_0}C_{M,q_j}$$

$\overline{\Delta p}(\xi,\eta,t)$, $\Delta p(\theta,\eta,t)$ local pressure difference between top and bottom surfaces of wing, positive down, lb/sq ft

$q_j(t)$ generalized coordinate of jth degree of freedom (as a subscript, q_j replaced by α denotes pitching, q_j replaced by ϕ denotes flapping, and q_j replaced by x^2 denotes parabolic camber deformation), $\bar{q}_j e^{i\omega t}$, ft

S area of wing surface, sq ft

s ratio of wing semispan to root semichord, l/b_0

t time, sec

V velocity of airstream, ft/sec

$\bar{w}(x,y)$ amplitude function of prescribed downwash, $w(x,y,t)=\bar{w}(x,y)e^{i\omega t}$, ft/sec

x,ξ chordwise coordinates referred to b_0

$x_0=x-\xi$

y,η spanwise coordinates referred to l

z vertical coordinate (sketch 1)

$\beta=\sqrt{1-M^2}$

δ spanwise interval between integration stations in region of span which contains control point

ζ semispan of region which contains control point (sketch 4)

θ angular chordwise variable (eq. (7) and sketch 2)

$$\theta_x=\cos^{-1}\left[\frac{b_0}{b}(\xi_m-x)\right]$$

Λ angle of sweep of quarter-chord line, measured from perpendicular to stream direction, positive clockwise, deg

λ taper ratio, $\dfrac{\text{Tip chord}}{\text{Root chord}}$

μ model mass ratio (mass of model divided by mass of air in a circular cone with local diameter equal to local chord of model)

$\xi_{le}(\eta), \xi_{te}(\eta), \xi_m(\eta)$ coordinates of leading edge, trailing edge, and midchord line, respectively

ρ air density, slugs/cu ft

ϕ generalized coordinate of angular displacement in flapping oscillation; as used herein, $\phi=\tan^{-1}\left(\frac{H_{tip}}{3l/2}\right)$

$\varphi_{L,q_j},\varphi_{M,q_j}$ phase angles between lift or pitching moment and displacement associated with jth mode of oscillation, deg; for example,

$$\varphi_{L,q_j}=\tan^{-1}\frac{(C_{L,q_j})_i}{(C_{L,q_j})_r}$$

ω angular frequency, radians/sec

ω_j angular frequency in jth mode, radians/sec

Indices:

i,r imaginary and real components

j mode of vibration under consideration

n,m chordwise and spanwise pressure modes, respectively, in aerodynamic quantities (see eq. (13))

x^2 indicates parabolic camber deformation

α indicates pitching

ϕ indicates flapping

THE INTEGRAL EQUATION RELATING LIFT AND DOWNWASH

The linearized boundary-value problem of determining the forces on a wing with either oscillatory or steady downwash conditions can be readily reduced to a problem of solving an integral equation that relates downwash and lift distribution. The purpose of this section is to introduce this equation and to cast it in a desirable working form.

PLAN FORM AND COORDINATE SYSTEM

Since the integral equation is derived in various publications (e.g., in refs. 20 and 21), the equation will not be rederived here but will be simply stated in terms of dimensionless coordinates that are particularly convenient for use in applications pertaining to flutter. In keeping with linear theory, the wing is considered as a plane impenetrable surface S that lies nearly in the xy-plane as indicated in sketch 1. In accordance with the common practice in analytical flutter studies of defining displacements and forces as positive downward, the z-axis is taken to be positive downward. Furthermore, the x,y,z coordinate system and the surface S are assumed to move in the negative x-direction at a uniform velocity V. It is remarked that the direction of the z-axis differs from that employed in other treatments (e.g., ref. 21) of the integral equation and its kernel function. This difference will be seen to lead to changes in sign in the kernel and in the relation between downwash and displacement when this procedure is compared with the treatments in references 14, 22, and 23.

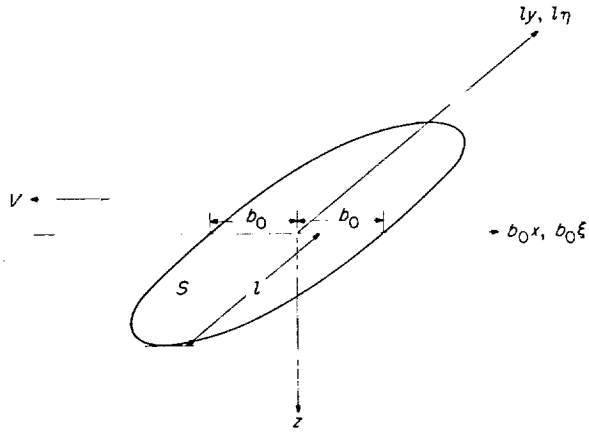

Sketch 1.

THE INTEGRAL EQUATION

With the considerations mentioned in the preceding section, a convenient form of the integral equation (obtained, e.g., from eq. (1) of ref. 21) may be formally written in terms of the unknown pressure distribution $\overline{\Delta p}(\xi,\eta,t)$ as

$$\frac{w(x,y,t)}{V}=\frac{b_0 l}{4\pi\rho V^2}\int_{-1}^{1}\int_{\xi_{le}(\eta)}^{\xi_{te}(\eta)}\overline{\Delta p}\,(\xi,\eta,t)\,K[M,k,x_0,s(y-\eta)]\,d\xi\,d\eta \quad (1)$$

where $w(x,y,t)$ is the vertical velocity or downwash at any point (x,y) on the wing, ρ is the fluid density, and $K[M,k,x_0,s(y-\eta)]$ is the kernel function of the integral equation. The quantity $K/4\pi\rho V$ (having the dimension of feet per second per pound) is the mathematical expression for the contribution to the downwash induced at any point (x,y) due to a unit force acting at any other point (ξ,η). In reference 21, K has been reduced to forms suitable for numerical evaluation. In equation (1), k is the reduced frequency $b_0\omega/V$; x_0 denotes the quantity $x-\xi$ in which x and ξ are dimensionless chordwise variables referred to the root semichord b_0; y and η are dimensionless spanwise variables referred to the semispan l, a convenient reference length in dealing with the span-

wise integration (note that this differs from the usage of ref. 21 in which y and η are referred to b_0); s is the ratio of semispan to root semichord l/b_0; and $\xi_{le}(\eta)$ and $\xi_{te}(\eta)$ are the chordwise coordinates of the leading and trailing edges, respectively.

A solution to the integral equation for a given plan form, a known mode of oscillation, and a given set of stream conditions requires a determination of the pressure distribution which will satisfy the edge conditions appropriate to the plan form and flow regime under consideration and which, when multiplied by the kernel function and integrated over the plan form, will yield the downwash distribution corresponding to the mode of oscillation. No means of solving the integral equation in an exact analytic sense has yet been found and it has therefore been necessary to resort to approximate or numerical procedures.

As stated in the introduction, a reliable concept on which to base an approximate solution to the integral equation involves expressing the unknown lift distribution as a sum of appropriately chosen modes of lift functions, each mode being weighted by a constant coefficient which must be determined. Employing this concept then allows the known downwash distribution to be expressed as a sum of definite integrals with the unknown coefficients appearing as factors of these integrals. Once the definite integrals are evaluated, the unknown coefficients can be readily determined by simple collocation.

In order to cast equation (1) in a useful working form it is convenient to consider first some desired forms of the various ingredients of the equation, namely, the downwash distribution, the lift distribution, and the kernel function.

FORM OF DOWNWASH DISTRIBUTION

In order to obtain a desired form of the downwash distribution for use in equation (1), it is assumed that the system under consideration is undergoing a displacement $H(x,y,t)$ which may be represented by a superposition of either natural or assumed modes of vibration so that

$$H(x,y,t)=h_1(x,y)\,q_1(t)+h_2(x,y)\,q_2(t)+\ldots +h_j(x,y)\,q_j(t)+\ldots \quad (2)$$

where, for sinusoidal oscillations,

$$q_j(t)=\overline{q}_j e^{i\omega t} \quad (3)$$

specifies the magnitude of the displacement in the jth mode, ω is the frequency of oscillation, and $h_j(x,y)$ gives the shape of the mode.

The downwash $w(x,y,t)$ associated with the displacement $H(x,y,t)$ is given by

$$w(x,y,t)=\left(\frac{V}{b_0}\frac{\partial}{\partial x}+\frac{\partial}{\partial t}\right)H(x,y,t) \quad (4)$$

or, with the use of equation (2),

$$\frac{w(x,y,t)}{V}=\left(\frac{\partial}{\partial x}+ik\right)\left[h_1(x,y)\,\frac{q_1(t)}{b_0}+h_2(x,y)\,\frac{q_2(t)}{b_0}+\cdots\right] \quad (5)$$

In application, each mode shape appearing in equation (5) will be handled separately. For convenience the downwash associated with the jth mode may be defined as

$$\frac{w_j(x,y,t)}{V}=\left(\frac{\partial}{\partial x}+ik\right)h_j(x,y)\,\frac{q_j(t)}{b_0} \quad (6)$$

FORM OF LIFT DISTRIBUTION

The choice of the lift functions selected to express the unknown pressure distribution should, of course, be made with discretion because the more compatible these functions are with the actual loading the fewer will be required. As a guide in selecting modes of lift, the character of the lift distribution, at least in the neighborhood of the wing edges, can be surmised from a knowledge of the few exact solutions to lifting-surface problems. For subsonic flow, the pressure or lift distribution on a wing should tend to zero along trailing edges and edges parallel to the stream direction as $\lim_{\epsilon\to 0}\sqrt{\epsilon}$, where ϵ is the distance to the wing edge. At the leading edge, the pressure or lift should behave as $\lim_{\epsilon\to 0}\frac{1}{\sqrt{\epsilon}}$. A summation of modes that satisfies these conditions and is otherwise perfectly general is employed, for example, in references 10, 13, and 14 and is used in the present development.

Before introducing this summation of modes, it is convenient to introduce an angular chordwise variable θ, shown in sketch 2.

The functions $\xi_{le}(\eta)$, $\xi_m(\eta)$, and $\xi_{te}(\eta)$ in sketch 2 represent equations of the leading edge, midchord line, and trailing edge, respectively. It

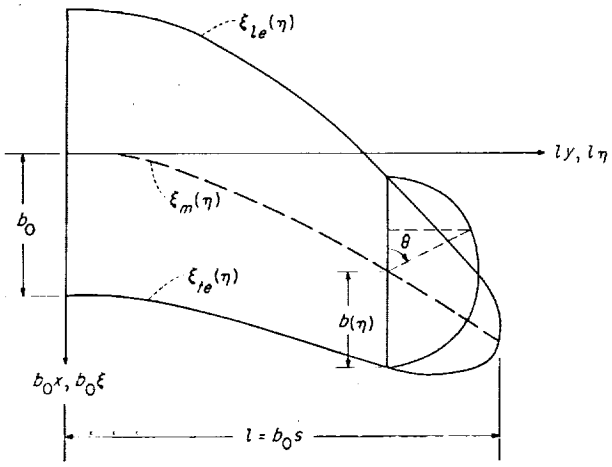

Sketch 2.

is noted that they may apply to plan forms with curved edges as well as to those with straight edges. The chordwise coordinate ξ may be expressed in terms of $\xi_m(\eta)$, b/b_0, and θ through the relation

$$\xi=\xi_m-\frac{b}{b_0}\cos\theta \qquad (0\leqq\theta\leqq\pi) \tag{7}$$

Note that ξ_m and b/b_0 can be readily expressed in terms of $\xi_{le}(\eta)$ and $\xi_{te}(\eta)$ as

$$\left.\begin{aligned}\xi_m&=\frac{\xi_{te}+\xi_{le}}{2}\\ \frac{b}{b_0}&=\frac{\xi_{te}-\xi_{le}}{2}\end{aligned}\right\} \tag{8}$$

The assumed pressure distribution of references 10, 13, and 14 employs the angular chordwise variable θ and is of the form

$$\overline{\Delta p}(\xi,\eta,t)=\Delta p(\theta,\eta,t)=4\pi\rho V^2\frac{l}{b_0}L(\theta,\eta)\frac{q(t)}{b_0} \tag{9}$$

where

$$\begin{aligned}L(\theta,\eta)=\frac{b_0}{b}\sqrt{1-\eta^2}\Big[&(a_{00}+\eta a_{01}+\eta^2a_{02}+\ldots)\cot\frac{\theta}{2}\\&+(a_{10}+\eta a_{11}+\eta^2a_{12}+\ldots)\sin\theta+\ldots\\&+\frac{4}{2^{2n}}(a_{n0}+\eta a_{n1}+\eta^2a_{n2}+\ldots)\sin n\theta+\ldots\Big]\end{aligned} \tag{10}$$

in which the coefficients a_{nm} are unknown weighting factors to be determined. (The factor $\frac{4}{2^{2n}}$ of $\sin n\theta$, not employed in the cited references, is used here for convenience.)

Equation (10) can be written more concisely by grouping the chordwise and spanwise pressure modes to obtain

$$L(\theta,\eta)=\frac{b_0}{b}\sum_n l_n(\theta)A_n(\eta) \tag{11}$$

in which

$$\left.\begin{aligned}l_0(\theta)&=\cot\frac{\theta}{2} \qquad (\eta=0)\\ l_n(\theta)&=\frac{4}{2^{2n}}\sin n\theta \quad (\eta\geqq 1)\end{aligned}\right\} \tag{12}$$

and in which

$$\begin{aligned}A_n(\eta)&=\sqrt{1-\eta^2}(a_{n0}+\eta a_{n1}+\ldots+\eta^m a_{nm}+\ldots)\\&=\sqrt{1-\eta^2}\sum_m\eta^m a_{nm}\end{aligned} \tag{13}$$

Note that in dealing with symmetric loading, only even powers of η are retained in equation (13); in dealing with antisymmetric loading, only odd powers of η are retained. For either symmetric or antisymmetric loading, as will be observed in the collocation procedure to be used, it is necessary to consider control points on only one wing panel.

It is remarked further that equations (7), (8), and (12) may be used to obtain the following corresponding algebraic forms of the chordwise pressure modes:

$$\left.\begin{aligned}l_0(\theta)=\bar{l}_0(\xi)&=\sqrt{\frac{\xi_{te}-\xi}{\xi-\xi_{le}}}\\ l_1(\theta)=\bar{l}_1(\xi)&=\frac{b_0}{b}\sqrt{\left(\frac{b}{b_0}\right)^2-(\xi_m-\xi)^2}\\ l_2(\theta)=\bar{l}_2(\xi)&=\frac{1}{2}\left(\frac{b_0}{b}\right)^2(\xi_m-\xi)\sqrt{\left(\frac{b}{b_0}\right)^2-(\xi_m-\xi)^2}\end{aligned}\right\} \tag{14}$$

and so forth. For application to the special case of surfaces with straight leading and trailing edges, the following definitions of ξ_{le} and ξ_{te} in terms of the span-to-chord ratio s, the taper ratio λ, and the sweep angle of the quarter-chord line Λ may be

useful:

$$\xi_{te}=-1+|y|\left(s\tan\Lambda+\frac{1-\lambda}{2}\right)$$

$$\xi_{te}=1+|y|\left[s\tan\Lambda-\frac{3(1-\lambda)}{2}\right]$$

Equation (9) and the associated definitions constitute a useful form of the assumed pressure distribution. In order to proceed toward a working form of equation (1), it remains to consider the form of the kernel function.

FORM OF KERNEL FUNCTION

A satisfactory working form of the kernel function is obtained from the expression for this function that is given by equation (D8) of reference 21. For later considerations it is convenient to have the kernel function expressed in a separated form as

$$K[M,k,x_0,s(y-\eta)]=\frac{\overline{K}[M,k,x_0,s(y-\eta)]}{b_0^2s^2(y-\eta)^2} \qquad (15)$$

where $\overline{K}$ denotes a modified form of the kernel function obtained by extracting from K the factor $\frac{1}{b_0^2s^2(y-\eta)^2}$. As may be noted, this factor can give rise to a second-order singularity and, hence, necessitate use of the concept of the "finite part of infinite integrals" in integrations involving the kernel function. For the oscillatory case the modified kernel function $\overline{K}$ is defined as

$$\overline{K}[M,k,x_0,s(y-\eta)]=e^{-ikx_0}\left\{-iks|y-\eta|+ks|y-\eta|K_1(ks|y-\eta|)+\frac{i\pi}{2}ks|y-\eta|\left[I_1(ks|y-\eta|)-L_1(ks|y-\eta|)\right]+\right.$$

$$\left.\frac{x_0e^{\frac{ik}{\beta^2}\left[x_0-M\sqrt{x_0^2+\beta^2s^2(y-\eta)^2}\right]}}{\sqrt{x_0^2+\beta^2s^2(y-\eta)^2}}-iks|y-\eta|\int_0^{\frac{1}{\beta^2s|y-\eta|}\left[x_0-M\sqrt{x_0^2+\beta^2s^2(y-\eta)^2}\right]}\frac{\tau}{\sqrt{1+\tau^2}}e^{iks|y-\eta|\tau}d\tau\right\} \qquad (16)$$

where K_1 and I_1 are modified Bessel functions and L_1 is a modified Struve function. For the steady case ($k=0$) the modified kernel function $\overline{K}$ is defined as

$$\overline{K}[M,0,x_0,s(y-\eta)]=1+\frac{x_0}{\sqrt{x_0^2+\beta^2s^2(y-\eta)^2}} \qquad (17)$$

Examination of $\overline{K}$ shows that it contains no infinite singularities but does possess one finite singularity when $x_0=y-\eta=0$. This singularity leads to no special difficulty, however, since it can be handled by making use of the following limiting forms of $\overline{K}$:

$$\left.\begin{aligned}\lim_{y-\eta\to0}\overline{K}[M,k,x_0,s(y-\eta)]&=2e^{-ikx_0} \qquad (x_0>0)\\ \lim_{y-\eta\to0}\overline{K}[M,k,x_0,s(y-\eta)]&=0 \qquad (x_0<0)\end{aligned}\right\} \qquad (18)$$

Equation (15) and the associated definitions of equations (16), (17), and (18) constitute the desired working form of the kernel function for use in the integral equation. (Note that in the definition of the kernel the sign differs from that given in ref. 21. This is a consequence of the convention used herein that forces are positive downward.)

Before returning to the integral equation it is desirable to discuss means of evaluating some of the functions which appear in equation (16). First, the integral will be treated; then, the Bessel function $K_1(ks|y-\eta|)$ and the combined function $I_1(ks|y-\eta|)-L_1(ks|y-\eta|)$ will be discussed.

The integral in $\overline{K}$.—It has not been possible to evaluate the integral which appears in equation (16) in an exact analytical sense. Although this integral is of a simple type for numerical integration, its evaluation can become time consuming or burdensome, particularly when the upper limit becomes large. In the present procedure an approximate, but accurate, alternative approach has been adopted.

By examination of equation (16) it may be seen that if $x_0>Ms|y-\eta|$, the upper limit of the integral is positive, but if $x_0<Ms|y-\eta|$, the upper

limit is negative. For present purposes it is desirable to express the integral in a form such that the integration extends only over positive ranges. The integral is thus expressed as

$$\int_0^{a-d} \frac{\tau}{\sqrt{1+\tau^2}} e^{iks|y-\eta|\tau} d\tau \qquad (x_0 > Ms|y-\eta|) \quad (19)$$

and

$$\int_0^{d-a} \frac{\tau}{\sqrt{1+\tau^2}} e^{-iks|y-\eta|\tau} d\tau \qquad (x_0 < Ms|y-\eta|) \quad (20)$$

where

$$a = \frac{x_0}{\beta^2 s|y-\eta|}$$

and

$$d = \frac{M\sqrt{x_0^2+\beta^2 s^2(y-\eta)^2}}{\beta^2 s|y-\eta|}$$

With these forms, the approach is to approximate a part of the integrand by the following expression, which applies for all positive values of τ:

$$\frac{\tau}{\sqrt{1+\tau^2}} \approx 1 - 0.101e^{-0.329\tau} - 0.899e^{-1.4067\tau} - 0.09480933e^{-2.90\tau}\sin \pi\tau \quad (21)$$

The expressions which result when equation (21) is substituted into equations (19) and (20) are readily integrable in closed form. The results have been incorporated into the computing program of the present procedure and need not be written here.

The approximation given by equation (21) has the same value as $\frac{\tau}{\sqrt{1+\tau^2}}$ at the two limits $\tau=0$ and $\tau=\infty$. The maximum deviation of the approximation from the value of $\frac{\tau}{\sqrt{1+\tau^2}}$ is about 0.24 percent in the vicinity of $\tau=1.5$.

The Bessel and Struve functions.—For values of $ks|y-\eta|>0$ the modified Bessel function $K_1(ks|y-\eta|)$ is evaluated by use of series expressions contained in a computing routine provided through an organization called SHARE made up of users of the IBM 704 and 709 electronic data processing machines. When $ks|y-\eta|=0$ the product $ks|y-\eta|K_1(ks|y-\eta|)$ has a limiting value of unity.

The combined quantity I_1-L_1 can be replaced by a definite integral, a convenient form of which is obtained from a general expression for $I_\nu-L_\nu$ given in reference 24 (p. 425). For the special case $\nu=1$ this definite integral is

$$I_1(ks|y-\eta|)-L_1(ks|y-\eta|) = \frac{2ks|y-\eta|}{\pi}\int_0^{\pi/2} e^{-ks|y-\eta|\cos\alpha}\sin^2\alpha\, d\alpha = \frac{2ks|y-\eta|}{\pi}\int_0^1 \sqrt{1-\tau^2}e^{-ks|y-\eta|\tau}d\tau \quad (22)$$

Either of the integrals in this equation can be readily evaluated by numerical integration methods to any desired degree of accuracy or, alternatively, an approximation to the integrand can be used which is integrable in closed form. The latter procedure has been employed in the present program because it is more economical of computing time and is believed to be sufficiently accurate. It has led to the following expression:

$$I_1(ks|y-\eta|)-L_1(ks|y-\eta|) \approx \frac{2ks|y-\eta|}{\pi}\left\{\frac{1.0085\, ks|y-\eta|}{1.3410+1.0050\, k^2s^2(y-\eta)^2} + \left[\frac{\pi}{4}-0.8675\, ks|y-\eta| \left(\frac{0.4648+0.9159\, ks|y-\eta|}{1.3410+k^2s^2(y-\eta)^2}\right)\right]e^{-ks|y-\eta|}\right\} \quad (23)$$

The error of this approximation reaches a maximum of about 0.4 percent in the vicinity of $ks|y-\eta|=4$ and is less for both smaller and larger values of the argument. The overall effect of this error in the whole problem is minor.

An idea of the general character of the kernel $\overline{K}$ can be had by examining the curves shown in figure 1. In this figure the real and imaginary parts of $\overline{K}$ are plotted against kx_0 for several constant values of $ks|y-\eta|$. The particular values shown are for a Mach number of 0.8. The significant features of these curves are the finite discontinuity at $ks|y-\eta|=kx_0=0$ and the rapid variations in $\overline{K}$ near $kx_0=0$ especially for small values of $ks|y-\eta|$. As will be seen, this behavior of the kernel necessitates special handling of the chordwise integrations over a range of values of $ks|y-\eta|$ near $y-\eta=0$.

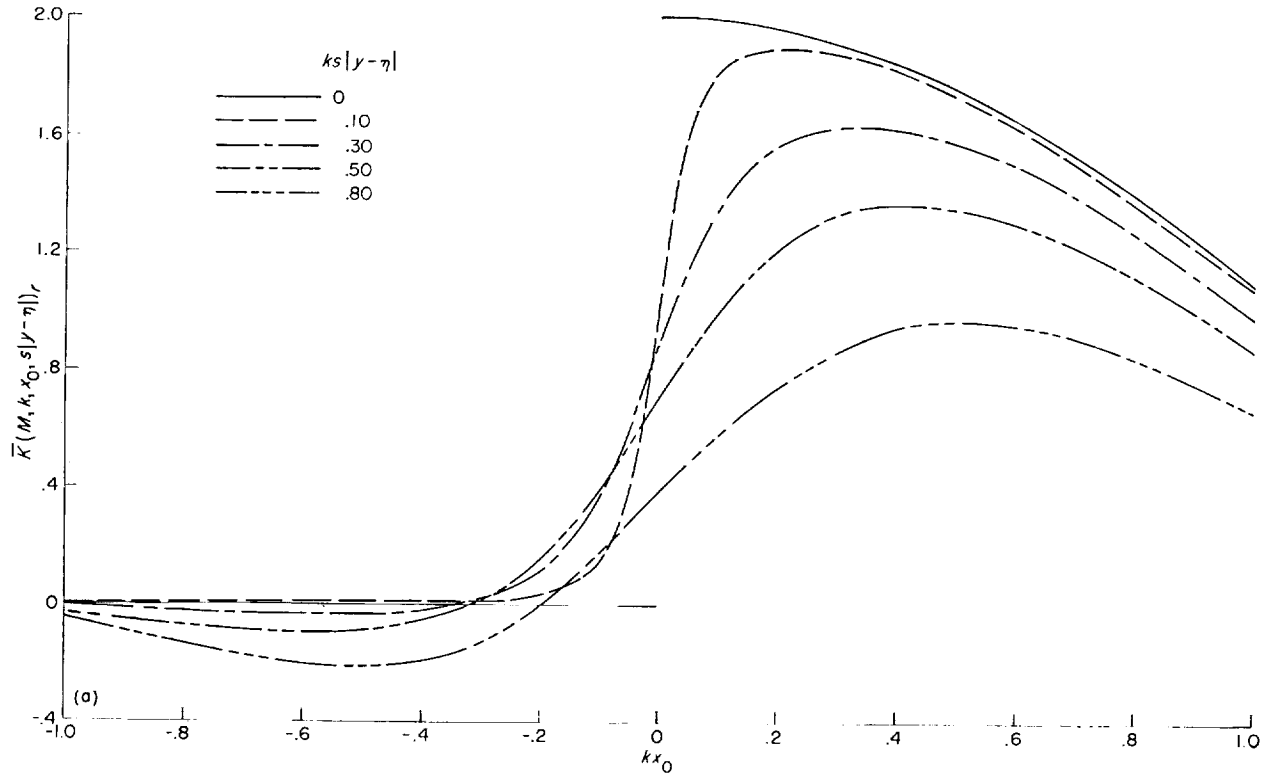

(a) Real part.

FIGURE 1.—Variation of modified kernel function $\overline{K}(M,k,x_0,s|y-\eta|)$ with kx_0 for various values of $ks|y-\eta|$. $M=0.8$.

WORKING FORM OF THE INTEGRAL EQUATION

The desired working form of the integral equation (eq. (1)) is readily obtained by employing the various ingredients in the forms arrived at in the preceding sections. By making use of the downwash as expressed by equation (5), the lift distribution as expressed by equation (9), and the kernel function as expressed by equation (15), the integral equation may be written for the jth mode of oscillation as

$$\frac{\overline{w}(x,y)}{V}=\left(\frac{\partial}{\partial x}+ik\right)h_j(x,y)$$
$$=\fint_{-1}^{1}\frac{b}{b_0}\frac{d\eta}{(y-\eta)^2}\int_0^{\pi}L_j(\theta,\eta)\overline{K}_\theta(M,k,\theta,\eta)\sin\theta\,d\theta \quad (24)$$

where

$$\overline{K}_\theta(M,k,\theta,\eta)=\overline{K}\left[M,k,\left(x-\xi_m+\frac{b}{b_0}\cos\theta\right),s(y-\eta)\right]$$

As was remarked earlier, the presence of the second-order singularity $\frac{1}{(y-\eta)^2}$ necessitates the use of the concept of the finite part of infinite integrals indicated in equation (24) by the notation $\fint$. The concept, as here employed, is discussed, for example, in references 11 and 25. Thus, the value of the improper integral $\int_a^b\frac{F(\eta)d\eta}{(y-\eta)^2}$ for $a<y<b$ is obtained from the following limit:

$$\fint_a^b\frac{F(\eta)d\eta}{(y-\eta)^2}=\lim_{\epsilon\to 0}\left[\int_0^{y-\epsilon}\frac{F(\eta)d\eta}{(y-\eta)^2}+\int_{y+\epsilon}^{b}\frac{F(\eta)d\eta}{(y-\eta)^2}-\frac{2}{\epsilon}F(y)\right] \quad (25)$$

Equation (24) together with equation (25) constitutes the desired working form of the integral equation. The subscripts j on the modal function h and on the lift function L in equation (24) indicate that a solution for the pressure distribution must be obtained for each individual mode of oscillation. In the discussions to follow, this will

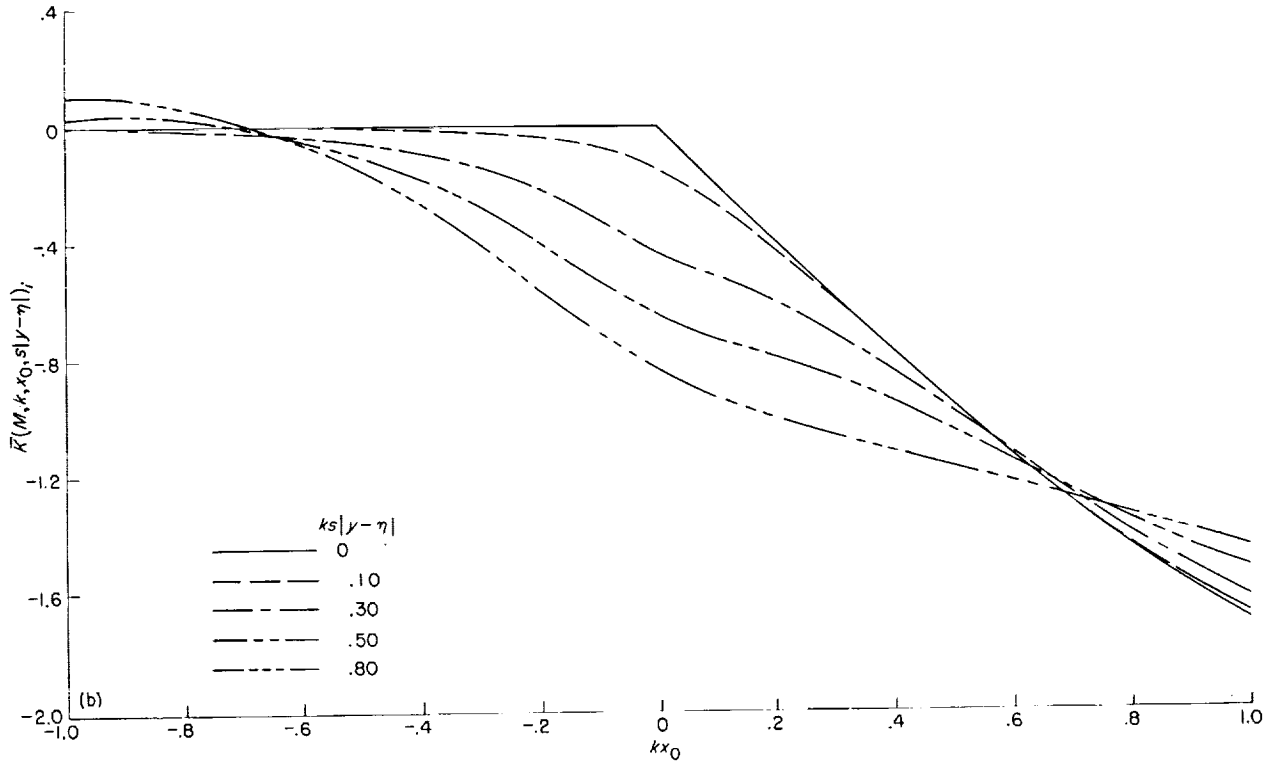

(b) Imaginary part.

FIGURE 1.—Concluded.

be understood to be the case and the subscripts will be dropped.

SOLUTION OF THE INTEGRAL EQUATION

When the expression for $L(\theta,\eta)$ given by equation (10) or (11) is substituted into equation (24), the downwash is expressed as the following sum of definite integrals:

$$\frac{\overline{w}(x,y)}{V}=\sum_n \sum_m a_{nm} \int_{-1}^{1} \frac{\eta^m\sqrt{1-\eta^2}\,d\eta}{(y-\eta)^2} \int_0^{\pi} l_n(\theta)\overline{K}_\theta(M,k,\theta,\eta)\sin\theta\,d\theta \quad (26)$$

The next problem, then, is one of devising a practical scheme for accurately evaluating the integrals.

The scheme of integration which has been devised is simple in principle but because of the many operations and parameters involved, it represents such a task of calculation that it is feasible only with the use of high-speed computing equipment. It is well suited for such equipment, however, and once it is programed the approximate lift distribution or its various integrated properties can be generated for a series of given mode shapes in a very few minutes.

In discussing the procedure it is convenient to separate the chordwise and spanwise integral operations and to write equation (26) as

$$\frac{\overline{w}(x,y)}{V}=\int_{-1}^{1} \frac{F(\eta)d\eta}{(y-\eta)^2} \quad (27)$$

where

$$F(\eta)=\sum_n \sum_m a_{nm}\eta^m\sqrt{1-\eta^2}f_n(\eta) \quad (28)$$

The function $f_n(\eta)$ in equation (28) is the chordwise integral and is defined by

$$f_n(\eta)=\int_0^{\pi} l_n(\theta)\overline{K}_\theta(M,k,\theta,\eta)\sin\theta\,d\theta \quad (29)$$

EVALUATION OF THE CHORDWISE INTEGRAL

The integrals defined by equation (29) involve no infinite singularities and can therefore be readily evaluated by numerical means to any desired degree of accuracy. In selecting specific integration

procedures to be employed, the characteristics of the integrand should, of course, be kept in mind and provision should be made for handling certain special situations. Specifically, proper account must be taken of the finite discontinuity in the kernel function at $x_0=y-\eta=0$, indicated by equation (18), and of the rapid variation in the kernel near $x_0=0$ for small values of $ks|y-\eta|$, indicated in figure 1.

In the present procedure these characteristics of the kernel are taken into account by performing the chordwise integration in two steps for certain ranges of values of $ks|y-\eta|$. For this purpose equation (29) is written as

$$f_n(\eta)=\int_0^{\theta_x} l_n(\theta)\overline{K}_\theta(M,k,\theta,\eta)\sin\theta\, d\theta + \int_{\theta_x}^{\pi} l_n(\theta)\overline{K}_\theta(M,k,\theta,\eta)\sin\theta d\theta \quad (30)$$

where θ_x denotes the value of θ which corresponds to $x_0=0$. The value of θ_x to be used in equation (30) can be obtained from equation (7) as

$$\theta_x=\cos^{-1}\left[\frac{b}{b_0}(\xi_m-x)\right] \quad (31)$$

By closely spacing the integration stations in each integral of equation (30) in the vicinity of the end point θ_x (as is done, e.g., in a Gaussian procedure), the rapid variation in the kernel can be more accurately handled.

An appropriate range of values of $ks|y-\eta|$ over which to employ the two-part chordwise integral (eq. (30)) can be arrived at by examining plots like those of figure 1. In the present procedure equation (30) is being handled by two 10-point Gaussian integrations in the region $ks|y-\eta|\leqq 0.3$. For larger values of $ks|y-\eta|$, the chordwise integrals are being evaluated by use of equation (29), with a single 10-point Gaussian integration. The computing program of the present procedure is extremely flexible with regard to the number of integration stations employed and can be easily modified.

One remark concerning the application of equation (30) to swept configurations is perhaps pertinent. When a control point is near a leading or trailing edge, it is possible for the line $\xi=x$ or $x_0=0$ to intersect the edge within the range of η values in which the two-part chordwise integration is used. In this event the argument of the inverse cosine in equation (31) will exceed ± 1.0. In the computing program of the present procedure provision is made for testing the argument of the inverse cosine and for performing the chordwise integration in one part, by use of equation (29), wherever $\frac{b}{b_0}|\xi_m-x|>1.0$.

Some sample values of chordwise integrals obtained by the present procedure are shown in figure 2. The figure shows the products of the factor $\sqrt{1-\eta^2}$ and the chordwise integrals $f_0(\eta)$,

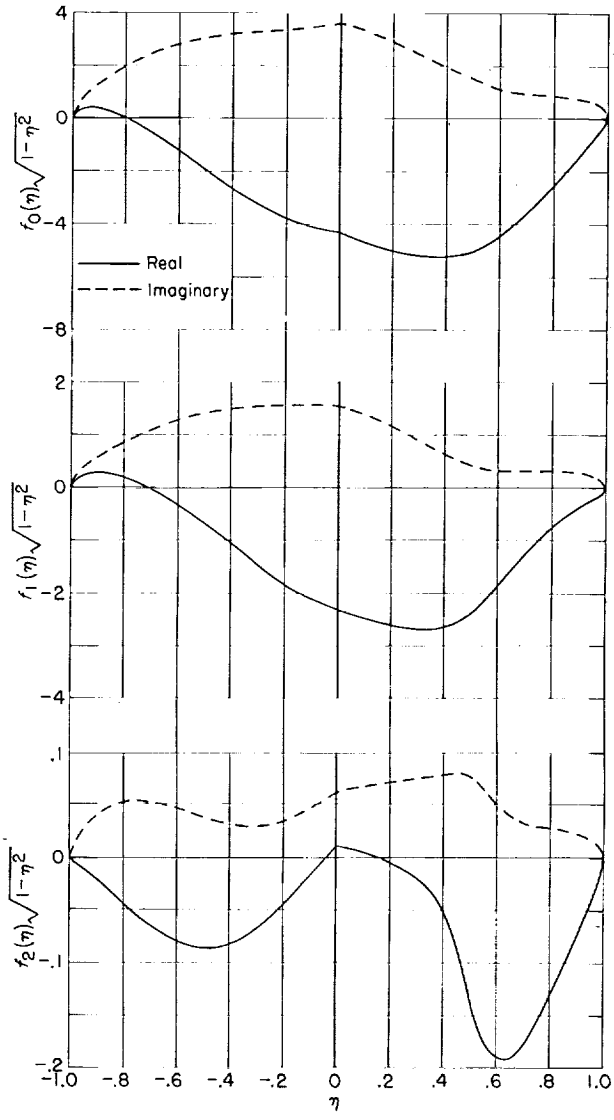

FIGURE 2.—Variation of chordwise integrals $f_n(\eta)$ (eq. 29) with η for a control point at $\eta=0.5$ on a swept tapered wing. $M=0.84$; $k=0.3$; $A=3.3$.

$f_1(\eta)$, and $f_2(\eta)$, defined by equations (29) and (30). These products are shown as functions of η for a tapered wing with straight edges. Note that for this case there is a discontinuity in slope of the curves at $\eta=0$ which is due to the factor b_0/b in the lift function $L(\theta,\eta)$. This factor is the ratio of root chord to local chord and, for the type of plan form treated, is discontinuous in slope at the wing root.

It is remarked that in earlier unpublished versions of the present procedure the chordwise integrals have been expressed in terms of the algebraic form of the chordwise pressure modes $\bar{l}_n(\xi)$, defined by equation (14). The first mode $\bar{l}_0(\xi)$ contains a singularity at the leading edge which can be handled by subtraction and addition in the integrand of the corresponding chordwise integral. This is a straightforward step but it leaves the integrand with infinite slope at the point where the singularity existed. As is well known, for integration of such shapes, closely spaced integration stations in the vicinity of the infinite slope are needed to approach exact results. Use of the angular variable θ, together with Gaussian integration procedures, should yield more accurate results for a given number of integration stations.

THE SPANWISE INTEGRATION

In order to accomplish the spanwise integration it is convenient to divide the wing into several regions as indicated in sketch 3.

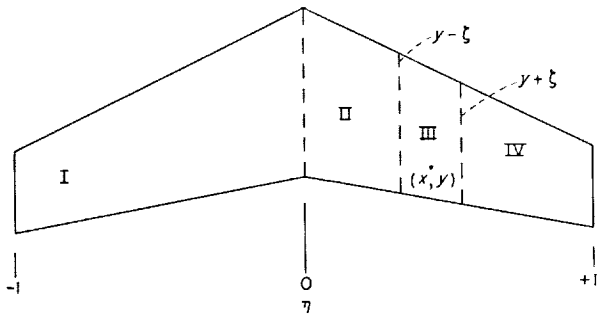

Sketch 3.

Region I extends from $\eta=-1$ to $\eta=0$ and is employed to take into account a possible discontinuity in slope at $\eta=0$ which may arise from the factor b_0/b as indicated in the preceding section. Region III extends a short distance ζ on each side of y, that is, from $\eta=y-\zeta$ to $\eta=y+\zeta$. The integrand of equation (27) for this region contains the second-order singularity $\frac{1}{(y-\eta)^2}$; hence, this region is intended to facilitate the evaluation of the finite part of the improper integral. Region II simply fills the gap between regions I and III and is absorbed into region III in cases for which the control point is in the neighborhood of $\eta=0$. Region IV fills the gap between region III and $\eta=1.0$ and is absorbed into region III in cases for which the control point is near a wing tip. Note that the function $F(\eta)$ in regions I and IV is characterized by an infinite slope at the wing tips which arises from the factor $\sqrt{1-\eta^2}$.

In conformity with the four regions just discussed, the spanwise integral can be written as

$$\int_{-1}^{1}\frac{F(\eta)d\eta}{(y-\eta)^2}=I_{\mathrm{I}}+I_{\mathrm{II}}+I_{\mathrm{III}}+I_{\mathrm{IV}} \tag{32}$$

where

$$I_{\mathrm{I}}=\int_{-1}^{0}\frac{F(\eta)d\eta}{(y-\eta)^2} \tag{33a}$$

$$I_{\mathrm{II}}=\int_{0}^{y-\zeta}\frac{F(\eta)d\eta}{(y-\eta)^2} \tag{33b}$$

$$I_{\mathrm{III}}=\fint_{y-\zeta}^{y+\zeta}\frac{F(\eta)d\eta}{(y-\eta)^2} \tag{33c}$$

$$I_{\mathrm{IV}}=\int_{y+\zeta}^{1}\frac{F(\eta)d\eta}{(y-\eta)^2} \tag{33d}$$

First, the evaluation of the integrals I_{I}, I_{II}, and I_{IV} will be discussed. Then, the integral I_{III}, which contains the singularity, will be treated.

The integrals I_{I}, I_{II}, and I_{IV} are not singular and can be readily evaluated by numerical means. In the present procedure the function $F(\eta)$ at each integration station within a particular region is evaluated from equation (28), divided by the appropriate value of $(y-\eta)^2$, and weighted by the integrating factor for the station. Thus, the integral I_{I}, for example, is expressed as

$$I_{\mathrm{I}}=\sum_{\nu=1}^{N}A_\nu\frac{F(\eta_\nu)}{(y-\eta_\nu)^2} \tag{34}$$

where the constants A_ν are the integrating factors and η_ν indicates the coordinates of the integrating stations appropriate to the N-point integration rule being used.

With regard to appropriate values of N, it is remarked that in the present procedure the span-

wise integrals are also handled by Gaussian integration rules. The number of integration stations employed varies from region to region and depends on the spanwise position of the control points and on aspect ratio. For aspect ratios of the order of 4 or less, region I is being handled by a 10-point rule regardless of control-point location; region II is being handled by from a 3- to a 10-point rule, the number increasing as the control point is moved outboard; in region IV, even though the control point may be well outboard, at least a 5-point rule is used to handle the aforementioned infinite slope at the tip and the number of points is increased to 10 as the control point moves inboard. For wings of much higher aspect ratio the number of points used in all three of the regions should be increased. As in the case of the chordwise integrals, the spanwise-integration scheme of the present procedure is very flexible with regard to the number of integration steps employed and the number can be easily changed.

The integral I_{III}, which involves the singularity at $\eta=y$, is evaluated by employing a polynomial to approximate $F(\eta)$ over the region of integration. This procedure permits the singular parts of I_{III} to be completely isolated and easily handled. In the present scheme $F(\eta)$ is represented by a sixth-degree polynomial that is readily determined by use of Lagrange's interpolation formula and is

$$F(\eta)=\frac{1}{\delta^6}\sum_{p=0}^{6}\frac{(-1)^p}{p!(6-p)!}\frac{(\eta-y+3\delta)(\eta-y+2\delta)(\eta-y+\delta)}{\eta-y+(3-p)\delta}\times(\eta-y)(\eta-y-\delta)(\eta-y-2\delta)(\eta-y-3\delta)F_{p+1} \tag{35}$$

where δ is the station interval ($\delta=\zeta/3$) and F_{p+1} denotes the value of the chordwise integral at station $p+1$. These quantities are indicated in sketch 4.

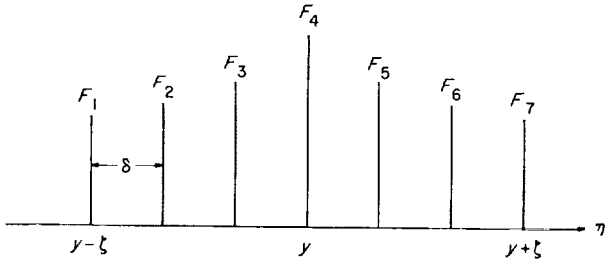

Sketch 4.

In order to accomplish the integration use is made of the identity $\eta=y-(y-\eta)$ so that the integral I_{III} can be written as

$$I_{III}=\int_{y-\zeta}^{y+\zeta}\frac{F(\eta)d\eta}{(y-\eta)^2}$$
$$\approx\frac{1}{\delta^6}\int_{y-\zeta}^{y+\zeta}[g_0(y-\eta)^4+\delta g_1(y-\eta)^3+\delta^2 g_2(y-\eta)^2+\delta^3 g_3(y-\eta)+\delta^4 g_4]d\eta+\frac{1}{\delta}g_5\int_{y-\zeta}^{y+\zeta}\frac{d\eta}{y-\eta}+g_6\int_{y-\zeta}^{y+\zeta}\frac{d\eta}{(y-\eta)^2} \tag{36}$$

where each term g is a certain linear combination of the ordinates of $F(\eta)$ and can be found by use of equation (35). For the present discussion only the final combination of the ordinates of $F(\eta)$ is of importance and the expressions for g need not be written.

The notation $\int$ in equation (36) is meant to imply that a Cauchy principal value of an integral is to be taken. For the integral involved the Cauchy principal value is

$$\int_{y-\zeta}^{y+\zeta}\frac{d\eta}{y-\eta}=\lim_{\epsilon\to 0}\left(\int_{y-3\delta}^{y-\epsilon}\frac{d\eta}{y-\eta}+\int_{y+\epsilon}^{y+3\delta}\frac{d\eta}{y-\eta}\right)$$
$$=\lim_{\epsilon\to 0}[\log 3\delta-\log\epsilon-\log(-3\delta)+\log(-\epsilon)]=0 \tag{37}$$

The last integral in equation (36) involves the singularity and is to be evaluated by use of the concept of the finite part of infinite integrals. Hence,

$$\int_{y-\zeta}^{y+\zeta}\frac{d\eta}{(y-\eta)^2}=\lim_{\epsilon\to 0}\left[\int_{y-3\delta}^{y-\epsilon}\frac{d\eta}{(y-\eta)^2}+\int_{y+\epsilon}^{y+3\delta}\frac{d\eta}{(y-\eta)^2}-\frac{2}{\epsilon}\right]$$
$$=\lim_{\epsilon\to 0}\left(\frac{1}{y-\eta}\Big|_{y-3\delta}^{y-\epsilon}+\frac{1}{y-\eta}\Big|_{y+\epsilon}^{y+3\delta}-\frac{2}{\epsilon}\right)=\frac{-2}{3\delta} \tag{38}$$

The nonsingular integral in equation (36) yields

$$\frac{1}{\delta^6}\int_{y-\zeta}^{y+\zeta}[g_0(y-\eta)^4+\delta g_1(y-\eta)^3+\delta^2 g_2(y-\eta)^2+\delta^3 g_3(y-\eta)+\delta^4 g_4]d\eta$$
$$=\frac{2}{15\delta}(729g_0+135g_2+45g_4) \tag{39}$$

Thus, combining equations (37), (38), and (39)

gives the integral I_{III} as

$$I_{III} \approx \frac{2}{15\delta}(729g_0+135g_2+45g_4-5g_6) \quad (40)$$

This result may be expressed in terms of the ordinates $F_1, F_2, \ldots F_7$ of $F(\eta)$ as

$$I_{III} \approx \frac{1}{300\delta}(13F_1+72F_2+495F_3-1{,}360F_4+495F_5 +72F_6+13F_7) \quad (41)$$

The complete spanwise integral is given by the sum of the results indicated by equation (34) for I_I, I_{II}, and I_{IV} and given by equation (41) for I_{III}. This sum expresses the downwash at the control point under consideration as a linear algebraic equation with the weighting factors a_{nm} as unknowns.

In order to determine the values of the unknown weighting factors a_{nm}, the simplest procedure is to select just as many control points as there are unknowns and to form and solve the set of simultaneous equations related to these points. This is an area where further work could be done in determining whether there is an optimum number of control points for a given problem or whether something like a least-squares approach might be useful. These questions are not settled here; some further remarks on the need for numerical research are given in the next section.

REMARKS ON THE METHOD

The purpose of this section is to indicate briefly some areas in which the need for further exploratory calculations and developments exists and to provide some remarks on the use of the present program.

AREAS FOR FURTHER NUMERICAL RESEARCH AND DEVELOPMENT

The development of the method presented herein has left untreated some questions and problems which may arise in applications and considerations of the procedure. Among these are the questions of optimum numbers or locations of control points or of the number of pressure modes necessary to assure satisfactory results for a given case.

Unfortunately, it is not possible, at least at this time, to give firm answers of general applicability to such questions. It appears unlikely that a general optimization of either control-point location or number of pressure modes is feasible but that each plan form and downwash distribution must be considered as a separate problem. It is hoped that for general applications optimization will not be necessary but that satisfactory accuracies can be obtained by employing a relatively few pressure modes along with a well-scattered pattern of control points.

A great deal seems to hinge on the accuracy with which the chosen lift functions represent the actual lift distribution for a particular problem. As the functions chosen to represent the lift become more and more realistic, the locations of control points should become less significant. The lift functions employed in the present procedure are chosen with a hope that the forms employed are at least near enough to reality to allow control points to be scattered in a pattern which is adequate for representing the downwash distributions encountered. Applications of the procedure to the circular (or elliptical) plan form, for which some results of analytic methods exist, might serve as the basis for studies of such questions.

While the computing program as it now exists is directly applicable to controls such as all-movable tails, there is a need for modifications and extensions that will make it applicable to controls in general. This would involve the determination of appropriate lift functions for handling various edge conditions which may be involved in control problems.

More experience is needed in applying the procedure to problems involving higher modes of oscillation and the associated higher frequencies. Presumably, for such problems, greater numbers of control points and lift functions would be needed. This, of course, implies an increase in the order of the matrices to be handled and may lead to formation of less well conditioned or even poorly conditioned matrices.

Some study is also needed to determine the benefits, if any, of the application of methods of weighting, such as least squares, that might permit evaluation of the unknown coefficients from a large number of control points rather than from the minimum number required.

COMPUTING PROCEDURE

As mentioned previously the procedure described herein has been programed for the IBM 704 electronic data processing machine. As presently programed, provision has been made for the inclusion of either three or four chordwise lift functions, together with either three or four

spanwise lift functions, in the series given by equation (10). This programing permits direct use of either 9, 12, or 16 control points.

The program proceeds in two steps: In one step the surface integrals associated with each control point and, thus, the coefficient matrix of the unknowns in the problem are generated; in the second step the coefficient matrix is inverted and combined with a number of sets of specified downwash conditions to obtain the weighting factors a_{nm} associated with each downwash condition. The two steps are separate so that should it be desired to apply, for example, a least-squares approach, as many equations as desired can be generated and an appropriate means of solving them provided.

In most of the calculations performed thus far, the usual practice has been to include three chordwise terms and three spanwise terms of equation (10) and to use these with just 9 control points. Usually the control points have been placed at or near the ¼-, ½-, and ¾-chord stations and at approximately the 0.2-, 0.5-, and 0.8-semispan stations. In the calculations described herein for the circular plan form, a very limited number of control-point variations have been attempted. Calculations have been made with 9 control points located as just described and with 9 control points arrayed as recommended in reference 11. Calculations have also been made with 12 control points by adding 1 control point at each of the three span stations used in the 9-point calculations and by distributing the points chordwise in the manner recommended in reference 11. In this limited study, results obtained for all coefficients varied by less than 2 percent.

The calculations consume about 25 seconds of machine time per control point when the numerical integrations are carried out with about the number of integration steps indicated in the text. Thus, about 4 minutes are required for the calculations with 9 control points. This time includes both program steps described in this section and involves the application of about five sets of downwash conditions in the second step.

The basic information provided by the computing program is a set of values of the pressure weighting factors a_{nm} for each prescribed downwash distribution. The program can be readily extended by the introduction of appropriate integrating matrices, and with very little increase in machine time, to yield any desired integrated property of the pressure distribution such as section or total lift and moment coefficients or the generalized forces required for flutter analysis.

NUMERICAL APPLICATIONS

In order to illustrate applications of the method, results of several calculations are presented. (Some of the results are taken from ref. 26; other results are as yet unpublished.) In the illustrations total forces and moments are compared (1) with results of analytic procedures for a circular plan form with steady downwash conditions, (2) with results of other theories and with experiments for a rectangular plan form of aspect ratio 1 at a uniform angle of attack, and (3) with some experimental results for a rectangular plan form of aspect ratio 2 undergoing pitching and flapping oscillations. Also included are results of flutter calculations compared with experiments for an all-movable control surface of aspect ratio 3.50 and for a cantilevered rectangular plan form of aspect ratio 5.04.

THE CIRCULAR PLAN FORM

Of the few plan forms for which analytical methods of treatment have been developed, one is the circular plan form. A compilation of results for the total lift and pitching moment on a circular plan form in steady incompressible flow is given in reference 9. The present procedure has been applied to this configuration with two distributions of downwash. These are for (1) an undeformed surface at constant angle of attack, defined by $h(x,y)=x$, and (2) a surface with parabolic camber deformation, defined by $h(x,y)=\frac{x^2}{2}$.

Total lift and pitching-moment coefficients and the location of the center of pressure have been obtained by the method presented herein and compared with results listed in reference 9 from the various analytic procedures. For the undeformed surface at constant angle of attack the results are as follows:

Source	$C_{L,\alpha}$	$C_{M,\alpha}$	Center of pressure, percent chord from leading edge
Kinner (ref. 27)	1. 8174	0. 9358	24. 75
Schade and Kriones (ref. 7)	1. 7984	. 9318	24. 60
Van Spiegel (ref. 9)	1. 7902	. 9326	23. 95
Present method	1. 7910	. 9389	23. 80

For the surface with parabolic camber deformation the following results have been obtained:

Source	C_{L,x^2}	C_{M,x^2}	Center of pressure, percent chord from leading edge
Kinner (ref. 27)	0. 9350	−0. 4376	26. 60
Schade and Krienes (ref. 7)	. 9436	−. 4382	26. 80
Van Spiegel (ref. 9)	. 9326	−. 4388	26. 45
Present method	. 9443	−. 4463	26. 40

The results of the present method differ by less than 2 percent from the results of the analytic procedures. All the results of the analytic procedures have been obtained by summing the first few terms of infinite series and, hence, are not exact. Were more terms of the series taken, or more significant figures carried in the calculations, the last figure shown (and possibly the last two figures) of the results of the analytic procedures might change.

THE RECTANGULAR PLAN FORM OF ASPECT RATIO 1

In reference 28 results from various theories have been collected and compared with an extrapolated experimental result for the total lift and center of pressure for a rectangular wing of aspect ratio 1.0 at a constant angle of attack. One of the tabulated results, obtained by use of the initial computing program of the present procedure, agreed poorly with the experimental result. In the initial program chordwise integrations were performed by use of Simpson's rule with rather widely spaced intervals. In addition, the chordwise lift distribution was expressed in algebraic form and the leading-edge singularity was extracted analytically. Such usage generally results in a small loss of accuracy arising from the infinite slope of the integrand at the leading and trailing edges. In this case there seems to have been a sensitivity to the loss of accuracy. The current computing program employs improved integration techniques and yields a considerably better result, as shown by the following comparison with some of the results of the various procedures listed in reference 28:

Source	C_{L,α_1}	Center of pressure, percent chord
Experiment (extrapolated) (ref. 28)	1. 400	16. 00
Jones (zero-aspect ratio) (ref. 29)	1. 570	0
Lawrence (ref. 30)	1. 400	17. 00
Hsu (ref. 19)	1. 497	14. 37
Present method (initial program)	1. 310	8. 79
Present method (current program)	1. 455	17. 21

THE RECTANGULAR PLAN FORM OF ASPECT RATIO 2—COMPARISON OF THEORETICAL AND EXPERIMENTAL AIR FORCES

The results of a number of experiments on simulated two-dimensional wing models (wings with end plates) are in good agreement with theoretical two-dimensional oscillating air forces, but relatively few experimental programs have been carried out to measure the air forces on oscillating finite wings. Among the few which do exist is a systematic series of tests on rectangular semispan wing models of aspect ratio 2. Two modes of oscillation have been studied: one, a pitching oscillation about an axis along the midchord, and the other, a flapping oscillation about an axis inboard of the wing root and parallel to the stream direction. The tests were conducted by two coordinated techniques with semirigid spring-mounted models. One technique was to force the model to oscillate; then, the resonant frequency was determined, the power input to the oscillator was obtained, and the lift forces were measured with strain gages. These values were compared with tare values determined from a resonant oscillation under vacuum conditions. The other technique was to oscillate the model at its resonant frequency, cut off the applied force, and record the decay of the motion. By testing over a range

of airspeed, results were obtained over a range of reduced frequency.

The pitching wing.—The experimental results for a midchord location of the pitch axis, obtained in reference 31, are presented in figure 3 and are compared with theoretical results for the kernel-function procedure. Figure 3(a) gives the amplitude and phase angle of the total lift coefficient $C_{L,\alpha}$ plotted against the reciprocal of k, the reduced frequency, and includes a sketch showing the semispan model, the pitch axis, and the tunnel wall. Figure 3(b) gives the amplitude and phase angle of the total pitching-moment coefficient $C_{M,\alpha}$. Also given along the abscissas of figures 3(a) and (b) are the test Mach numbers corresponding to various values of $1/k$. The theoretical curves were obtained by using the appropriate Mach number. The agreement of theory and experiment is generally good but the results in figure 3(b) show appreciable scatter in the data.

The flapping wing.—In figure 4 the results from reference 22 for a flapping mode of oscillation are shown. Amplitudes and phase angles for the total lift coefficient $C_{L,\phi}$ and the total pitching-moment coefficient $C_{M,\phi}$ (midchord axis) appear in figures 4(a) and 4(b), respectively, plotted against the reduced frequency k. Figure 4(a) also includes a sketch of the semispan model, tunnel wall, and the flapping axis behind the tunnel wall. The test Mach number ranged only up to 0.41 and, therefore, the theoretical curves were determined on the basis of $M=0$. The agreement of theoretical and experimental coefficient amplitudes is good and the phase-angle agreement ranges from good to fair. A considerable decrease in scatter of the experimental data in comparison with the data of figure 3 is evident and is believed to be the result of improved experimental technique and instrumentation achieved over a period of time.

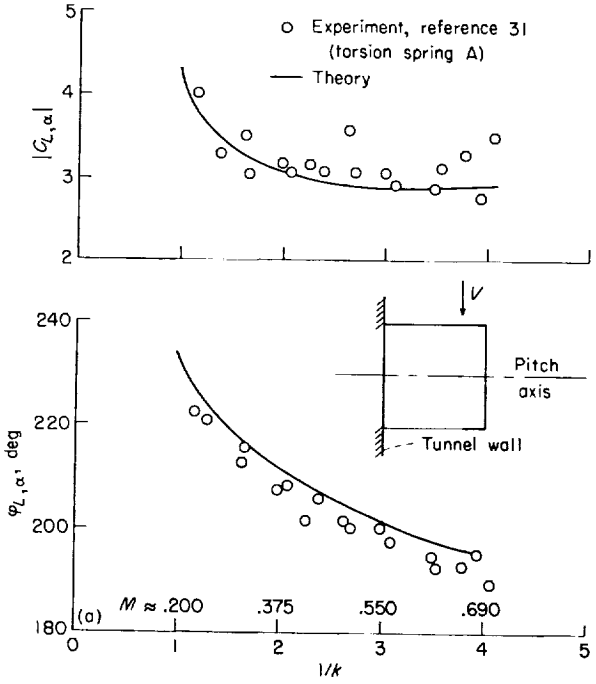

(a) Total lift coefficient.

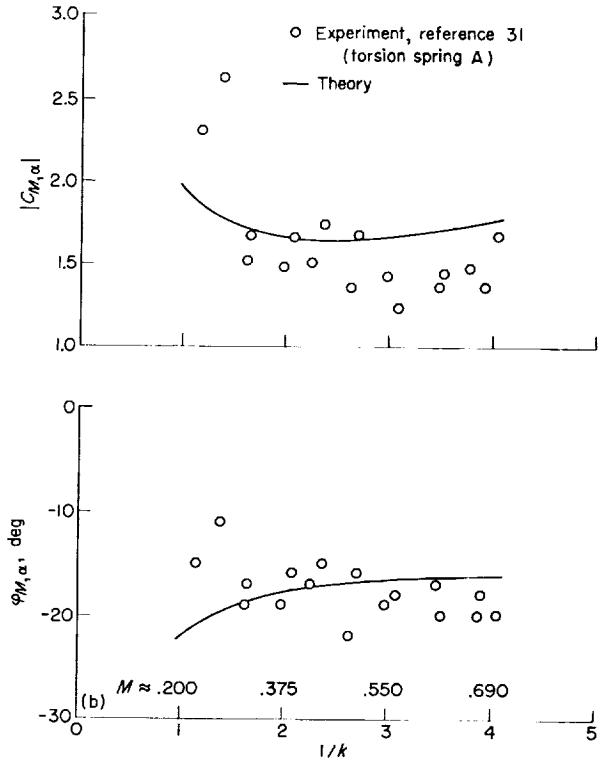

(b) Total pitching-moment coefficient.

FIGURE 3.—Concluded.

COMPARISON OF THEORETICAL AND EXPERIMENTAL FLUTTER RESULTS

A number of applications of the kernel function procedure have been made in calculating flutter boundaries, but relatively few published comparisons with experiment have been made available. One such comparison appears in reference 23 for a 45° delta semispan model mounted as a cantilever

FIGURE 3.—Comparison of theoretically and experimentally determined lift and pitching-moment coefficients (amplitudes and phase angles) plotted against $1/k$ for a rectangular wing of aspect ratio 2 oscillating in pitch about midchord.

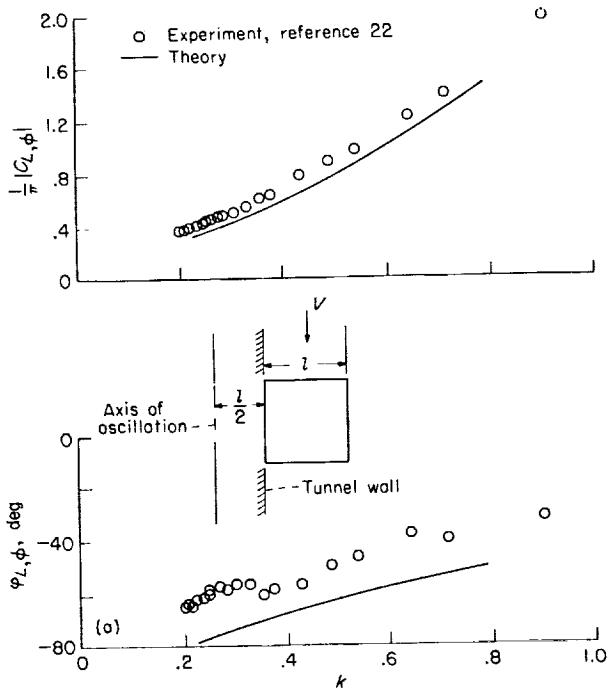

(a) Total lift coefficient.

FIGURE 4.—Comparison of theoretically and experimentally determined lift and pitching-moment coefficients (amplitudes and phase angles) plotted against k for a rectangular plan form of aspect ratio 2 undergoing a flapping oscillation.

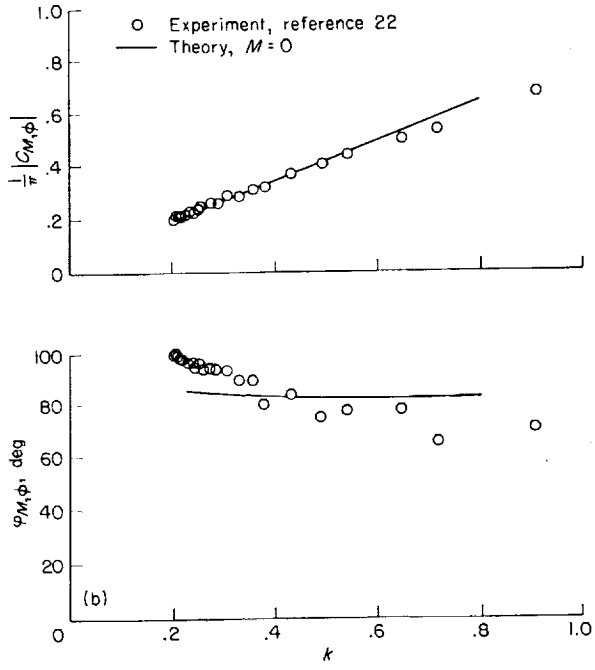

(b) Total pitching-moment coefficient.

FIGURE 4.—Concluded.

at its root and tested at $M=0.85$. In this study the theoretical boundary was found to be slightly conservative compared with the experimental boundary. Another comparison of theory and experiment, indicated in reference 26, is based on a series of flutter experiments carried out in the Langley 8-foot transonic pressure tunnel. The model, shown schematically at the top of figure 5, was a swept, tapered, all-movable control surface with an aspect ratio of 3.50. In figure 5 the flutter-speed ratio $\frac{V}{b_0\omega_2\sqrt{\mu}}$ and frequency ratio ω/ω_2 are plotted against M. The model mass ratio μ equals the mass of the model divided by the mass of the air in a truncated circular cone with the local diameter equal to the local chord of the model. The mass ratio μ is included in the flutter-speed ratio because wind-tunnel density had to be gradually changed in order to obtain flutter at different Mach numbers on the same model. The second

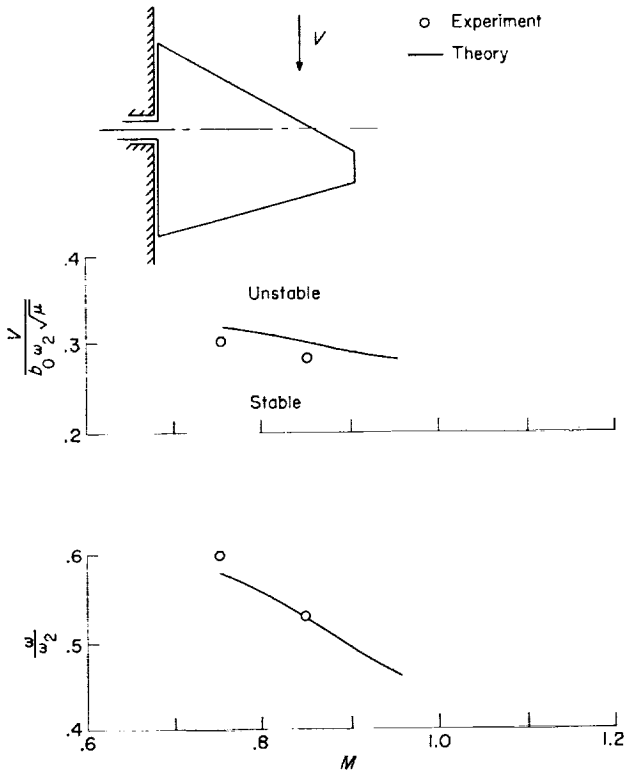

FIGURE 5.—Theoretically determined flutter-speed ratio $\frac{V}{b_0\omega_2\sqrt{\mu}}$ and flutter-frequency ratio ω/ω_2 plotted against M and compared with two flutter experiments on an all-movable control-surface model. (See ref. 26.) $\Lambda=20°$; $A=3.50$; $\lambda=0.15$.

natural frequency ω_2 is used because the second natural mode most nearly resembled a pure pitching mode. The theoretical results shown were obtained by using three natural modes. The speed ratio is unconservative by a few percent in comparison with the two experimental points shown; the flutter frequencies agree quite well.

Another comparison between theoretically and experimentally determined flutter characteristics is shown in figure 6 for a cantilever-mounted rectangular wing of aspect ratio 5.04. The experimental data in this figure represent a portion of the results of a series of tests presented in reference 32. In figure 6 the stiffness-altitude parameter $\frac{b_0\omega_2}{a}\sqrt{\mu}$ and frequency ratio ω/ω_2 are plotted against M. For the configuration of this example, the second natural mode of frequency ω_2 is essentially a pure torsion mode. The theoretical results shown were obtained by using the first three uncoupled modes of a uniform cantilever beam. For the range of Mach number over which comparisons are made, the theoretical values of the stiffness-altitude parameter agree very well with the experimental values; the theoretical values of the flutter-frequency ratio are within 10 percent of the experimental values.

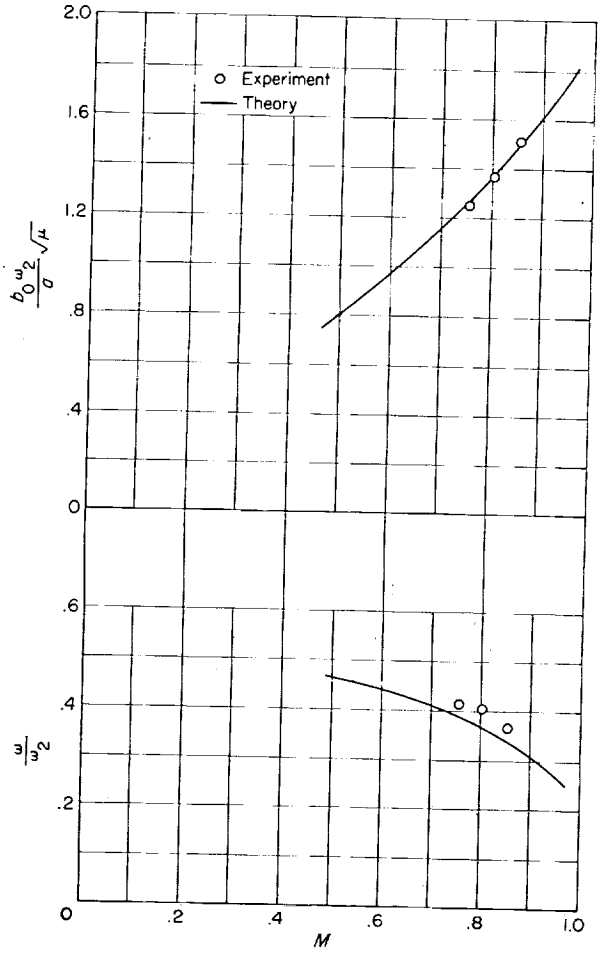

FIGURE 6.—Theoretically determined stiffness-altitude parameter $\frac{b_0\omega_2}{a}\sqrt{\mu}$ and flutter-frequency ratio ω/ω_2 plotted aganist M and compared with flutter experiments on a cantilever-mounted rectangular plan form of aspect ratio A of 5.04.

CONCLUDING REMARKS

A detailed description has been given of the numerical procedure employed in a solution of the integral equation which relates oscillatory or steady lift and downwash distributions on finite wings in subsonic flow. The procedure, which has been programed for the IBM 704 electronic data processing machine, is applicable to general plan forms with either curved or straight leading and trailing edges. While, as developed, the procedure is readily applicable to control surfaces such as all-movable tails, modifications are needed to apply it to controls in general.

The procedure has been applied to a number of examples, some of which deal with the determination of integrated aerodynamic forces and moments and some of which deal with applications to flutter problems. Integrated forces and moments obtained for a circular plan form are compared with results of analytical procedures for some steady downwash conditions; the results differ by less than 2 percent. Integrated forces and moments for rectangular plan forms are compared with experiment or with other theories for steady flow and for pitching and flapping oscillations. In each instance the results are in generally good agreement.

The flutter examples include comparisons of calculations with experiments for an all-movable control surface and for a rectangular wing of aspect ratio 5.04, both at high subsonic speeds. For both examples the theoretical results agree well with the experimental results.

LANGLEY RESEARCH CENTER,
NATIONAL AERONAUTICS AND SPACE ADMINISTRATION,
LANGLEY FIELD, VA., *June 2, 1959.*

REFERENCES

1. Theodorsen, Theodore: General Theory of Aerodynamic Instability and the Mechanism of Flutter. NACA Rep. 496, 1935.
2. Timman, R., and Van de Vooren, A. I.: Theory of the Oscillating Wing With Aerodynamically Balanced Control Surface in a Two-Dimensional, Subsonic, Compressible Flow. Rep. F.54, Nationaal Luchtvaartlaboratorium (Amsterdam), June 1949.
3. Possio, Camillo: The Aerodynamical Action on an Oscillating Aerofoil at Supersonic Speed. Rep. No. 7668, British A.R.C., May 3, 1944. (From Acta, Pont. Acad. Sci., vol. I, no. 11, 1937, pp. 93–106.)
4. Garrick, I. E., and Rubinow, S. I.: Theoretical Study of Air Forces on an Oscillating or Steady Thin Wing in a Supersonic Main Stream. NACA Rep. 872, 1947. (Supersedes NACA TN 1383.)
5. Garrick, I. E.: Some Research on High-Speed Flutter. Third Anglo-American Aero. Conf., Sept. 4–7, 1951 (Brighton, England). R.A.S., 1952, pp. 419–446J.
6. Merbt, H., and Landahl, M.: Aerodynamic Forces on Oscillating Low Aspect Ratio Wings in Compressible Flow. KTH Aero TN 30, Div. Aero., Roy. Inst. Tech. (Stockholm), 1953.
7. Schade, Th., and Krienes, K.: The Oscillating Circular Airfoil on the Basis of Potential Theory. NACA TM 1098, 1947.
8. Kochin, N. E.: Steady Vibrations of Wing of Circular Plan Form. Theory of Wing of Circular Plan Form. NACA TM 1324, 1953.
9. Van Spiegel, E.: Theory of the Circular Wing in Steady Incompressible Flow. NLL–TN F.189, Nationaal Luchtvaartlaboratorium (Amsterdam), Jan. 1957.
10. Falkner, V. M.: The Calculation of Aerodynamic Loading on Surfaces of Any Shape. R. & M. No. 1910, British A.R.C., Aug. 1943.
11. Multhopp, H.: Methods for Calculating the Lift Distribution of Wings (Subsonic Lifting Surface Theory). Rep. No. Aero. 2353, British R.A.E., Jan. 1950.
12. Possio, Camillo: Aerodynamic Forces on an Oscillating Profile in a Compressible Fluid at Sub-sonic Speed. Air Ministry Translation No. 830, British A.R.C., Nov. 24, 1938. (From Volume Commemorative del XXV Annuale del Laboratario di Aeronautica del R. Politecnico di Torino. Turin 14–17, Oct. 1937, pp. 152–169.)
13. Lehrian, Doris E.: Calculation of Flutter Derivatives for Wings of General Plan-Form. R. & M. No. 2961, British A.R.C., 1958.
14. Runyan, Harry L., and Woolston, Donald S.: Method for Calculating the Aerodynamic Loading on an Oscillating Finite Wing in Subsonic and Sonic Flow. NACA Rep. 1322, 1957. (Supersedes NACA TN 3694.)
15. Garner, H. C.: Multhopp's Subsonic Lifting-Surface Theory of Wings in Slow Pitching Oscillations. R. & M. No. 2885, British A.R.C., 1956.
16. Allen, D. J.: The Application of Multhopp's Subsonic Lifting Surface Theory to the Calculation of the Aerodynamic Forces Acting on a Wing of Finite Aspect Ratio Oscillating in Arbitrary Elastic Modes With Control Surface Freedom. Design Dept. Rep. No. 1191, Hawker Aircraft, Ltd. [Kingston-on-Thames, England], June 1953.
17. Richardson, J. R.: A Method for Calculating the Lifting Forces on Wings (Unsteady Subsonic and Supersonic Lifting Surface Theory). Tech. Office Rep. No. 165, The Fairey Aviation Co., Ltd. (Hayes, England), Apr. 1955.
18. Jordan, Peter F.: A Method for Determining Three-Dimensional Flutter Coefficients for Wings of Arbitrary Planform in Incompressible Flow. WADC Tech. Rep. 57–228, ASTIA Doc. No. AD 142309, U.S. Air Force, Jan. 1958.
19. Hsu, Pao-Tan: Flutter of Low-Aspect-Ratio Wings. Part I—Calculation of Pressure Distributions for Oscillating Wings of Arbitrary Planform in Subsonic Flow by the Kernel-Function Method. Tech. Rep. 64–1 (Contract No. NOa(s) 55–771–c), Aeroelastic and Structures Res. Lab., M.I.T., Oct. 1957.
20. Küssner, H. G.: General Airfoil Theory. NACA TM 979, 1941.
21. Watkins, Charles E., Runyan, Harry L., and Woolston, Donald S.: On the Kernel Function of the Integral Equation Relating the Lift and Downwash Distributions of Oscillating Finite Wings in Subsonic Flow. NACA Rep. 1234, 1955. (Supersedes NACA TN 3131.)
22. Woolston, Donald S., Clevenson, Sherman A., and Leadbetter, Sumner A.: Analytical and Experimental Investigation of Aerodynamic Forces and Moments on Low-Aspect-Ratio Wings Undergoing Flapping Oscillations. NACA TN 4302, 1958.
23. Woolston, Donald S., and Sewall, John L.: Use of the Kernel Function in a Three-Dimensional Flutter Analysis With Application to a Flutter-Tested Delta-Wing Model. NACA TN 4395, 1958.
24. Watson, G. N.: A Treatise on the Theory of Bessel Functions. Second ed., The Macmillan Co., 1944
25. Mangler, K. W.: Improper Integrals in Theoretical Aerodynamics. Rep. No. Aero. 2424, British R.A.E., June 1951.
26. Cunningham, Herbert J., and Woolston, Donald S.: Developments in the Flutter Analysis of General Plan Form Wings Using Unsteady Air Forces From the Kernel Function Procedure. Proc. Nat. Specialists Meeting on Dynamics and Aeroelasticity (Fort Worth, Texas), Inst. Aero. Sci., Nov. 1958, pp. 27–36.
27. Kinner, W.: Die kreisförmige Tragfläche auf potential theoretischer Grundlage. Ing.-Archiv, Bd. VIII, Heft 1, Feb. 1937, pp. 47–80.
28. Hsu, Pao-Tan: Some Recent Developments in the Flutter Analysis of Low-Aspect-Ratio Wings. Proc. Nat. Specialists Meeting on Dynamics and Aeroelasticity (Fort Worth, Texas), Inst. Aero. Sci., Nov. 1958, pp. 7–26.
29. Jones, Robert T.: Properties of Low-Aspect-Ratio

Pointed Wings at Speeds Below and Above the Speed of Sound. NACA Rep. 835, 1946. (Supersedes NACA TN 1032.)

30. Lawrence, H. R.: The Lift Distribution on Low Aspect Ratio Wings at Subsonic Speeds. Jour. Aero. Sci., vol. 18, no. 10, Oct. 1951, pp. 683–695.
31. Widmayer, Edward, Jr., Clevenson, Sherman A., and Leadbetter, Sumner A.: Some Measurements of Aerodynamic Forces and Moments at Subsonic Speeds on a Rectangular Wing of Aspect Ratio 2 Oscillating About the Midchord. NACA TN 4240, 1958. (Supersedes NACA RM L53F19.)
32. Doggett, Robert V., Jr., Rainey, A. Gerald, and Morgan, Homer G.: An Experimental Investigation of Aerodynamic Effects of Airfoil Thickness on Transonic Flutter Characteristics. NASA TM X–79, 1959.

U.S. GOVERNMENT PRINTING OFFICE: 1960